




# Complement inhibitor factor H expressed by breast cancer cells differentiates CD14<sup>+</sup> human monocytes into immunosuppressive macrophages

Karolina I. Smolag <sup>a</sup>, Christine M. Mueni<sup>a\*</sup>, Karin Leandersson<sup>a\*</sup>, Karin Jirström<sup>b</sup>, Catharina Hagerling <sup>c</sup>, Matthias Mörgelin<sup>d</sup>, Paul N. Barlow<sup>e</sup>, Myriam Martin<sup>a#</sup>, and Anna M. Blom <sup>a#</sup>

<sup>a</sup>Department of Translational Medicine, Lund University, Malmö, Sweden; <sup>b</sup>Department of Clinical Sciences, Lund University, Lund, Sweden; <sup>c</sup>Department of Laboratory Medicine, Lund University, Lund, Sweden; <sup>d</sup>Colzyx, Medicon Village, Lund, Sweden; <sup>e</sup>Edinburgh Biological NMR Unit, University of Edinburgh, Edinburgh, UK

## ABSTRACT

Macrophages are a major immune cell type in the tumor microenvironment, where they display a tumor-supporting phenotype. Factor H (FH) is a complement inhibitor that also plays a role in several cellular functions. To date, the phenotype of monocytes stimulated with FH has been unexplored. We discovered that FH is a survival factor for CD14<sup>+</sup> primary human monocytes, promoting their differentiation into macrophages in serum-free medium. This activity was localized to the C-terminal domains of FH and it was inhibited in plasma, indicating that the phenomenon may be most relevant in tissues. FH-induced macrophages display characteristics of immunosuppressive cells including expression of CD163 and CD206, release of the anti-inflammatory cytokine IL-10 and changes in metabolism. Furthermore, FH-induced macrophages express low levels of HLA-DR but high levels of co-inhibitory molecule programmed death-ligand 1 (PD-L1), and accordingly, a reduced capacity for T-cell activation. Finally, we show that FH is expressed by human breast cancer cells and that this correlates with the presence of immunosuppressive macrophages, breast cancer recurrence and severity of the disease. We propose that the expression of FH by tumor cells and the promotion of an immunosuppressive cancer microenvironment by this protein should be taken into account when considering the effectiveness of immunotherapies against breast cancer.

## ARTICLE HISTORY

Received 25 September 2019  
Revised 11 December 2019  
Accepted 14 December 2019

## KEYWORDS

Breast cancer; macrophages; factor H

## Introduction

Breast cancer is one of the most common health burdens worldwide claiming over 400,000 deaths every year. Progression of this malignancy is a complicated process regulated by tumor-immune cell interactions via cellular and molecular factors, systemically and in the tumor microenvironment.



Monocytes are a heterogeneous population of myeloid cells expressing high levels of CD14 (classical), CD16 (non-classical) or both markers (intermediate). Classical monocytes circulate in the blood where they undergo conversion into patrolling monocytes, become apoptotic<sup>1</sup> or transmigrate through endothelial tissues.<sup>2,3</sup> In tissues, monocytes can retain most of their transcriptional profile, gain antigen-presenting function and differentiate into macrophages, dendritic cells or monocytic myeloid-derived suppressor cells. Macrophages are often classified as M1 macrophages supporting inflammation<sup>4,5</sup> and M2 macrophages suppressing ongoing inflammation, facilitating remodeling and wound healing.<sup>6,7</sup> However, such binary classification does not adequately represent the observed heterogeneity of these cells and can be seen as two extremes of many intermediate phenotypes.<sup>6,8</sup>

Tumor-infiltrating myeloid cells, especially tumor-associated macrophages (TAMs), have a negative effect on breast cancer patients' survival<sup>9</sup> due to their ability to acquire

immunosuppressive functions, promoting angiogenesis and invasion.<sup>10-12</sup> The presence and type of TAMs have been linked with severity, prognosis and patient survival.<sup>13</sup> The development of new therapies targeting the cancer microenvironment is therefore of increasing interest.


Complement inhibitor factor H (FH) is mainly expressed in the liver, but also extrahepatically by various cell types, including ovarian<sup>14</sup> and lung<sup>15</sup> cancer cell lines. FH has been shown to affect myeloid cell functions not related to complement, including chemotactic effects on monocytes,<sup>16</sup> stimulation of prostaglandin E from perinatal macrophages<sup>17</sup> and restraining mononuclear phagocytes at the site of inflammation.<sup>18</sup> Previously, we revealed that opsonization with FH increased the clearance of apoptotic cell remnants and skewed the resultant cytokine production by phagocytes to an anti-inflammatory profile.<sup>19</sup>

Herein we establish that FH influences monocyte viability, differentiation and polarization, which for the first time defines FH as an inducer of primary human monocyte differentiation into immunosuppressive macrophages. Additionally, we propose that this new phenomenon is of importance in breast cancer, as we show that breast cancer FH expression positively correlates with the presence of immunosuppressive (CD163<sup>+</sup>) macrophages in human tumors.

**CONTACT** Anna M Blom  [anna.blom@med.lu.se](mailto:anna.blom@med.lu.se)  Department of Translational Medicine, Lund University, Inga Marie Nilsson's street 53, Malmö 214 28, Sweden

\*Shared second authors, contributing equally

#Shared last/senior authors, contributing equally

 Supplemental data for this article can be accessed on the [publisher's website](#).

© 2020 The Author(s). Published with license by Taylor & Francis Group, LLC.

This is an Open Access article distributed under the terms of the Creative Commons Attribution-NonCommercial License (<http://creativecommons.org/licenses/by-nc/4.0/>), which permits unrestricted non-commercial use, distribution, and reproduction in any medium, provided the original work is properly cited.

## Materials and methods

### Cells

Peripheral blood was collected from healthy volunteers with ethical approval (Dnr.2013/846, Dnr.2017/582). Cells were purified by density gradient centrifugation over LymphoPrep (#07811; Axis-Shield) followed by positive selection with CD14/CD16 microbeads for monocytes (#130-050-201, #130-045-701; Milteny Biotech) or CD4 for T-cells (#130-096-533; Milteny Biotech). Purity was assessed to >95%. Unless otherwise stated CD14<sup>+</sup> monocytes were used in the study. Monocytes were cultured in RPMI 1640 (#SH30027.01; GE Healthcare Life Sciences) for 48 h, and Macrophage-SFM medium (#11500426; Gibco) for 7 days, at density 1x10<sup>6</sup>/ml. Cells were stimulated with 150 µg/ml FH and α1-AT. For FH dose-dependence, monocytes were incubated for 96 h with 10, 20, 100 and 250 µg/ml of FH and cell length was assessed with ImageJ. Monocytes were also treated with 100 ng/ml of LPS (#L6386; Sigma-Aldrich) with or without 150 µg/ml of FH for 48 h. Macrophages were differentiated with FH, 25 ng/ml GM-CSF or 25 ng/ml M-CSF (#11343123, #11343113; ImmunoTools) for 7 days. Fully polarized proinflammatory and immunosuppressive macrophages we obtained by stimulation for 7 days with 25 ng/ml GM-CSF and 100 ng/ml of LPS for the last 4 h or by stimulation for 7 days with 25 ng/ml M-CSF and 20 ng/ml IL-4 and IL-13 (#11340047, #11340133; ImmunoTools) for the last 3 days, respectively. All the incubations were done in 37°C and 5% CO<sub>2</sub>. Human Jurkat T-cells were rendered apoptotic using 1 µM staurosporine (#37,095; Sigma-Aldrich). Mouse bone marrow cells were isolated from femur bone of four sacrificed C57BL/6 mice and incubated with 150 µg/ml FH for 6 days (ethical approval #M123-15). All the bright light images were taken with an EVOS inverted microscope (Thermo Fisher Scientific).

### Proteins and nucleosomes

FH<sup>20</sup> and α1-AT<sup>21</sup> were purified from human plasma (at least 95% pure). LPS contamination was tested using a Limulus amoebocyte lysate Endochrome-K assay (#R1708K; Charles River) and levels have been determined to <0.01–0.03 EU/ml in working concentration for FH and <0.04 for α1-AT. FH was incubated for 30 min at 96°C to obtain D-FH.<sup>22</sup> FH CCP1-7 and CCP19-20 were produced in *Pichia pastoris*.<sup>23</sup> Nucleosomes were isolated with Nucleosome preparation kit (#53504; Active Motif) and labeled in parallel with Jurkat T-cells with pHrodo ester (#P35369; Invitrogen).

### Cytokine profiling

Monocytes were incubated for 48 h or 7 days in medium with or without FH or α1-AT, macrophages were obtained as above. LPS was added to indicated samples for the last 15 h. Supernatants were analyzed using the Bio-Plex Pro human cytokine 27-plex assay and IL-10 ELISA (#M500KCAF0Y, #HS100C; R&D systems). For statistical calculations in Figure 5e, the data below detection limit were replaced with 10% of the lowest point on the standard curve.

### Phagocytosis assay

pHrodo green-labeled nucleosomes, apoptotic cells, pHrodo green-labeled *Staphylococcus aureus* particles, and zymosan (#P35367, #P35365; Invitrogen) were fed for 1 h to monocytes pre-incubated for 48 h with FH or α1-AT; or to macrophages obtained as above. Live cells were visualized with Calcein Violet AM (#C34858; Invitrogen) and fluorescence intensity was measured in Cytation-5 multi-mode reader (BioTek).

### Real-time quantitative PCR (RT-PCR)

TaqMan gene expression assays (Applied Biosystems) were performed according to the manufacturer's instruction. Gene expression was calculated using the ΔCt method.<sup>24</sup> Primers used for qPCR: TREM2 (#Hs00219132\_m1), MSR1 (#Hs00234007\_m1), MMP7 (#Hs01042796\_m1), IL1R2 (#Hs00174759\_m1), PPIA (#Hs99999904\_m1) and HPRT1 (#Hs99999909\_m1).

### Affymetrix array

RNA from monocytes of six donors incubated for 48 h with or without FH had an RNA quality indicator of at least 8.3 (Experion RNA chip; Bio-Rad). RNA was hybridized with the Affymetrix Clariom D chip. Data were normalized using the Robust MultiChip Averaging algorithm.<sup>25</sup> All arrays were quality controlled by the visual inspection of MDS- and MA-plots. To identify differentially expressed genes, a linear model was fitted, using donor as a blocking factor and treatment as the main outcome. To adjust for multiple testing the Benjamini and Hochberg method was applied<sup>26</sup> and q-values <0.05 were considered significant with no cutoff for fold change. For gene-set analysis, we applied the Generally Applicable Gene-set Enrichment methodology.<sup>27</sup> All microarray data and metadata are available under accession number GSE129670 (<https://www.ncbi.nlm.nih.gov/geo/query/acc.cgi?acc=GSE129670>).

### Confocal microscopy

Monocytes attached to Ibidi 8-well chamber slide (#80,841; Ibidi) were incubated with FH for 5, 15 or 30 min, fixed with 4% paraformaldehyde (#100,496; Merck) and permeabilized with 0.5% Triton X-100 (#T8787; Sigma-Aldrich). Cells were blocked with 5% normal donkey serum and donkey anti-goat Alexa Fluor 647, donkey anti-rat Alexa Fluor 488, donkey anti-rabbit Alexa Fluor 594 (#017-000-121, #705-606-147, #712-546-153, #711-585-152; Jackson ImmunoResearch), goat anti-human FH antiserum (#A312; Quidel), rabbit anti-human EEA1 and rat anti-human CD44 (#PA1-063A, #MA4400; Invitrogen), normal rabbit or goat IgG control sera (#AB-105-C, #AB-108; R&D Systems), were applied. Nuclei were visualized with DAPI mounting medium (#P36971; Molecular probes). All samples were analyzed in an LSM 510 Meta confocal microscope using 63x objective and Zen 2009 software (Zeiss). The degree of co-localization was estimated using CoLocalizer Express.

### Cell fractionation

Monocytes were incubated for 30 min in PBS with or without biotinylated FH. Cells were lysed with NP-40 lysis buffer supplemented with Pierce protease inhibitor mini tablets (#88666; Thermo Scientific) and Halt phosphatase inhibitor cocktail (#78420; Thermo Scientific). Cell fractionation was performed using Mem-PER Plus protein extraction kit (#89842; Thermo Scientific). FH was detected with Streptavidin-HRP (#DY998; R&D Systems) and endosomes with rabbit anti-human EEA1 antibody (#PA1-063A; Invitrogen). For fractionation controls, mouse anti-human  $\beta$ -actin (#ab8226; Abcam) and mouse anti-human E-cadherin (#610182; BD) were used.

### Arginase activity

Monocytes were incubated for 7 days in medium. Macrophages were obtained as above. Arginase activity assay (#ab180877; Abcam) was performed according to the manufacturer's instructions.

### Viability

Monocytes were incubated with or without FH or  $\alpha$ 1-AT for a total of 8 days, followed by the addition of Sytox green (#S7020; Thermo Fisher Scientific). Alternatively, monocytes were incubated with or without 150  $\mu$ g/ml FH,  $\alpha$ 1-AT and HI-FH for 4 days followed by 2 h incubation with Alamar blue (#DAL1100; Invitrogen). Fluorescence intensity was measured in Cytation-5 multi-mode reader (BioTek). For determination of cell viability by SEM, monocytes were incubated with or without 150  $\mu$ g/ml FH for 2 and 6 days.

### Flow cytometry

For analysis of surface markers and cell size and granularity, monocytes were incubated for 7 days in medium or  $\alpha$ 1-AT, macrophages were differentiated as above, and dendritic cells were differentiated with 5 ng/ml GM-CSF and 20 ng/ml IL-4. Surface markers were determined with mouse anti-human CD68-PE, mouse anti-human CD163-APC, mouse anti-human CD206-APC, mouse anti-human CD86-PE (#IC20401P, #FAB1607A, #FAB25342A; R&D Systems), mouse anti-human CD11c-APC, mouse anti-human PD-L1-APC, mouse anti-human CD1a-PE (#559877, #563741, #555807; BD), mouse anti-human HLA-DR-PE, mouse anti-human CD80-AF647, (#FAB4869P, #MCA2071A647; Bio-Rad) and mouse anti-human DC-Sign-AF647 (#32,501; Serotec) antibodies. Before staining with anti-CD68, cells were permeabilized with Cytotfix/Cytoperm (#554722; BD). For measurement of T-cell proliferation, cells were stimulated with 10 or 100 ng/ml of staphylococcal enterotoxin A and toxic shock syndrome toxin-1 (#S9399-1MG, #T5662-1MG; Merc). Autologous carboxy-fluorescein succinimidyl ester (#21888; Sigma-Aldrich) labeled CD4<sup>+</sup> T-cells were added for 96 h. Signal was measured in a Cytotflex flow cytometer (Beckman Coulter) and analyzed with FlowJo software (Tree Star). Pictures of cells were taken and sizes of the clusters were measured with ImageJ.

### Immunohistochemical staining

HEK 293 cells were transfected with FH full-length cDNA cloned in pcDNA3. Wild-type (WT) and FH-transfected 293 cell pellets were embedded in paraffin and sectioned. Tissue microarrays included biopsies from breast cancer patients (144 women) with ethical permission (ref. no. 445/2007). Tissue microarrays and controls were pre-treated using the PT-link system (Dako) with antigen retrieval at pH 6 and stained with goat anti-human FH antiserum (#A312; Quidel), mouse anti-human L20/3 (#sc-47686; Santa Cruz Biotechnology) and MRC-OX24 (ECACC Hybridoma Collection) for 30 min. The intensity of the staining in tumor cells was scored from 0 (negative) to 3 (high) by three researchers in a blinded manner. HER2 expression, hormone receptor status and Ki-67 were predetermined for the cohort.<sup>28-30</sup>

### Statistical analyses

Statistical analyses were performed in Prism (GraphPad) or SPSS Statistics (IBM). Data are presented as mean  $\pm$  SD and analyzed with one-way ANOVA, two-way ANOVA or Kruskal-Wallis with Tukey's multiple comparison test, Bonferroni multiple comparison test, Dunn's multiple comparison test or Friedman test. Survival was assessed using Kaplan-Meier analyses with Breslow test. Correlations of FH expression and clinical parameters were calculated with Mann-Whitney *U*-test or two-tailed Spearman rank-order correlation test. *P*-values <0.05 denoted statistical significance and are displayed as \**P* < 0.05, \*\**P* < 0.01, \*\*\**P* < 0.001.

## Results

### FH induces changes in monocyte morphology and viability

Primary human CD14<sup>+</sup> monocytes were cultured for 48 h in serum-free RPMI medium, supplemented with purified FH, alpha-1 antitrypsin ( $\alpha$ 1-AT) as negative control or heat-denatured FH (D-FH). FH-treated monocytes displayed markedly different morphologies than cells incubated in medium only or  $\alpha$ 1-AT. FH-treated cells were elongated, larger and more strongly attached. This effect was dose dependent (Figure S1A&B) and denaturation of FH abolished the morphological changes (Figure 1a). Endotoxin contamination of FH was negligible (<0.03 EU/ml) and monocytes stimulated with LPS alone did not undergo similar morphological changes as observed for FH-treated cells (Figure S1C) confirming that the FH effect is not related to potential LPS contamination.

Higher cell viability was detected for monocytes treated with FH than for cells cultured in  $\alpha$ 1-AT or medium only (Figure 1b). Increased viability of FH-treated cells after 48 h incubation was confirmed with alamar blue assay and scanning electron microscopy (SEM) (Figure S1D&E). Mouse bone marrow-derived progenitor cells treated for 6 days with FH also showed cell elongations and increased attachment suggesting higher viability (Figure 1c) indicating that the phenomenon is not limited to man.

SEM analyses confirmed higher circularity (Figure 1d,j), fewer elongations (Figure 1d,k) and smaller cell areas

## Monocytes (48 h)

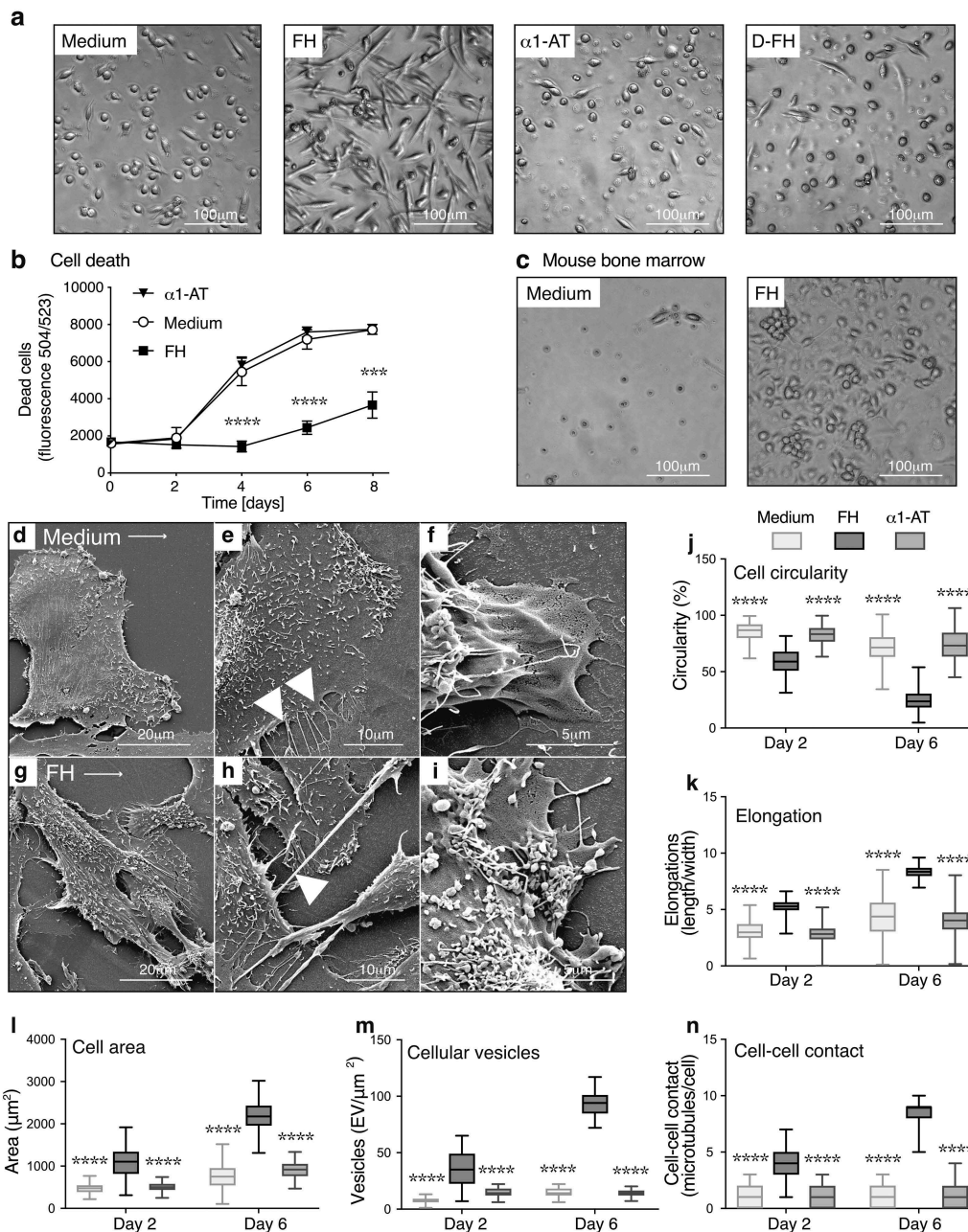


**Figure 1.** FH changes the morphology and prolongs the viability of monocytes.

(a) Morphological changes in human peripheral blood  $\text{CD14}^+$  monocytes upon incubation for 48 h with RPMI 1640 medium, 150  $\mu\text{g}/\text{ml}$  FH,  $\alpha$ 1-AT or heat-denatured FH. (b) Cell death assessed by Sytox green inclusion of monocytes incubated with medium, 150  $\mu\text{g}/\text{ml}$  FH or  $\alpha$ 1-AT for 8 days. (c) Morphology of mouse bone marrow progenitor cells incubated with medium or 150  $\mu\text{g}/\text{ml}$  FH for 6 days. (d–i) Scanning electron microscopy of monocytes incubated with medium (d–f) or 150  $\mu\text{g}/\text{ml}$  FH (g–i) for 6 days. (j–n) Quantification of cell circularity (j), elongation (k), cell area (l), cellular vesicles (m) and cell-cell contact (n) of  $\text{CD14}^+$  monocytes cultured for 2 and 6 days in medium, 150  $\mu\text{g}/\text{ml}$  FH or  $\alpha$ 1-AT. Data are means  $\pm$  SD of  $n=500$  cells.

(Figure 1l) in human monocytes incubated for 48 h with the medium than in FH-treated cells (Figure 1g,j–l). Cells without FH exhibited only small membrane extrusions (Figure 1e,m) and their membranes were mostly smooth (Figure 1f,n), while FH-treated cells exhibited long, thin elongations responsible for cell-cell contacts (Figure 1h,n). An increased number of membrane-associated vesicles indicated a high level of metabolic activity (Figure 1i,m).

### FH-stimulated monocytes express macrophage-specific surface markers

Colony-stimulating factor (M-CSF) and granulocyte-macrophage colony-stimulating factor (GM-CSF) are widely used to differentiate monocytes into macrophages.<sup>6</sup> M-CSF differentiated cells are referred to as immunosuppressive and GM-CSF differentiated cells as proinflammatory macrophages.<sup>31</sup> M-CSF macrophages additionally activated with interleukin

4 (IL-4) and IL-13 are denoted M2 and GM-CSF macrophages activated with LPS as M1.

The morphology of FH-stimulated cells more closely resembled immunosuppressive than proinflammatory macrophages (Figure 2a). The size (FSC) and granularity (SSC) of FH-treated monocytes exhibited high similarity to macrophages, but not to medium (Figure 2b) or  $\alpha$ 1-AT (Figure S1F) incubated monocytes.

Monocytes were differentiated for 7 days with FH and compared to immunosuppressive and proinflammatory macrophages as well as to monocytes cultured without stimuli. FH-induced macrophages displayed a similar expression level of CD163, CD11c, CD206 and CD68 (Figure 2c–f) as well as of CD80, CD86 and CD16 (Figure S2A) as immunosuppressive and proinflammatory macrophages, whereas cells cultured in medium only expressed lower levels of all markers. The possibility that FH induces differentiation of monocytes into dendritic cells (DC) was excluded by the absence of the characteristic DC markers CD1a and DC-Sign (Figure S2B).

The phagocytic capacity of FH-induced macrophages showed a higher resemblance to immunosuppressive than to proinflammatory macrophages regarding uptake of apoptotic cells (Figure 2g) and nucleosomes (Figure 2h). Monocytes stimulated with FH for 48 h displayed an increased ability to phagocytize apoptotic cells (Figure 2j), nucleosomes (Figure 2k) and zymosan (Figure 2i,l) in comparison to medium only and  $\alpha$ 1-AT incubated monocytes, while the clearance of bacterial particles was not affected (Figure S2E).

### ***FH binds to the surface of primary monocytes and becomes internalized***

Confocal microscopy showed that after 5 min incubation, FH was bound to the cell surface of primary monocytes and colocalized with the membrane marker CD44 (Figure 3a). Since apoptotic cells internalize surface-bound FH,<sup>19</sup> we investigated whether this also occurs in viable monocytes. After 30 min incubation, a significant proportion of FH was detected intracellularly as displayed by the confocal XY image with an orthogonal view of the YZ dimension (Figure 3b). Internalization occurs via endocytosis, which was shown by colocalization of internalized FH with early endosome antigen 1 (EEA1) (Figure 3c). The Mander's overlap co-efficient for the FH/EEA1 staining was 0.55 indicating a large degree of colocalization.<sup>32</sup> Specificity of FH and EEA1 stainings was verified with normal IgG control sera (Figure S2C, D). Internalization was confirmed by detection of FH in the cytoplasmic fraction of the monocytes, which also contains endocytic vesicles as EEA1 was present in the same fraction (Figure 3d).

This suggests that FH itself might bind a cell surface receptor yet to be identified and induce intracellular signaling that results in monocyte differentiation.

### ***Only CD14<sup>+</sup> monocytes are differentiated upon stimulation with FH***

To study the susceptibility of different monocyte subtypes to FH stimulation, CD14<sup>+</sup> (used throughout the article) and

CD16<sup>+</sup> monocytes were stimulated with FH. Only CD14<sup>+</sup> monocytes, which include the classical (CD14<sup>+</sup>/CD16<sup>-</sup>) and intermediate (CD14<sup>+</sup>/CD16<sup>+</sup>) subsets, showed changes in morphology upon FH treatment. CD16<sup>+</sup> monocytes retained the typical round morphology of un-stimulated monocytes with only a few elongations (Figure 3e).

### ***FH CCP19-20 but not CCP1-7 domains are responsible for FH-mediated changes in monocyte morphology***

To assess which domains of FH are responsible for the changes in monocyte morphology, recombinant FH fragments consisting of the seven N-terminal complement control protein domains (CCPs), or the two C-terminal CCPs, were incubated with monocytes. CCP1-7 contains the domains responsible for the complement inhibitory properties of FH, while C-terminal CCP19-20 enables attachment of FH to host cell surfaces and interactions with sialic acid.<sup>33,34</sup> While CCP1-7 had no effect, the C-terminal fragment altered monocytes comparably to full-length FH (Figure 3f).

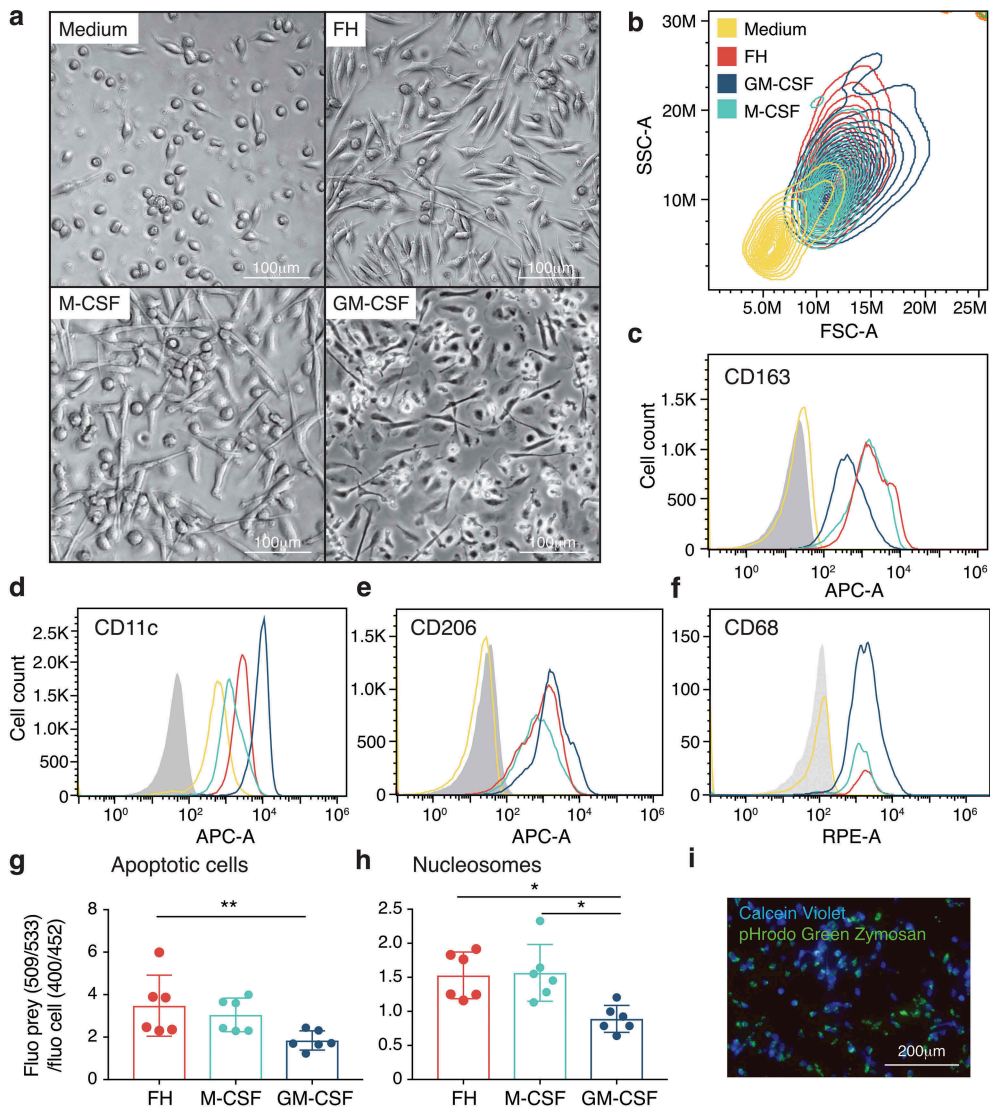
### ***Autologous plasma inhibits FH-mediated changes in monocyte morphology***

To study why the FH-induced morphological changes of monocytes do not occur in blood, where FH is most abundant, monocytes were incubated with FH and increasing concentrations of autologous plasma were added. Plasma inhibited the FH effect in a dose-dependent manner and at high plasma concentrations, the cells remained round and weakly attached (Figure 3g). This indicates that other plasma components inhibit or mask FH in the blood and that the differentiating phenomenon likely occurs only in tissues.

### ***FH alters the gene expression profile of monocytes at early differentiation stages***

To understand the early mechanisms underlying the effect of FH, we analyzed global mRNA expression changes using Affymetrix mRNA array. cDNA of monocytes from six donors incubated for 48 h with or without FH, was hybridized with Clariom D arrays. After adjustment for multiple testing, ten genes were identified with a false discovery rate (FDR)-corrected p-value <0.05, and 70 genes had a nominal p-value <0.0001 (Table S1). The most significantly regulated genes were visualized in a volcano plot (Figure 4a). Genes that were most upregulated by FH include interleukin 1 receptor 2 (IL1R2), matrix metalloproteinase 7 (MMP7) and N-myc downstream-regulated gene 2 (NDRG2), whereas macrophage scavenger receptor-1 (MSR1) and triggering receptor expressed on myeloid cells 2 (TREM2) were the most down-regulated genes upon FH stimulation (Figure 4a). Gene expression changes were validated in independent samples by real-time PCR, confirming FH-induced down- (MSR1 and TREM2) and upregulation (IL1R2 and MMP7) (Figure 4b). A heat map illustrates that FH-stimulated cells express higher levels of M2-related genes (Figure 4c). Interestingly, we found that FH affects many genes that are related to macrophage function in cancer (Figure 4d).

## Macrophages (7 days)



## Monocytes (48 h)

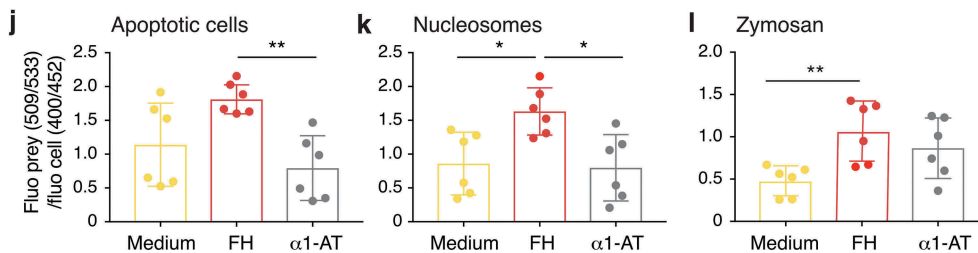


**Figure 2.** FH differentiates monocytes into macrophages.

Primary human CD14<sup>+</sup> monocytes were cultured for 7 days (a–h) or 48 h (i–l) with 150  $\mu$ g/ml FH, 150  $\mu$ g/ml  $\alpha$ 1-AT, 25 ng/ml GM-CSF or 25 ng/ml M-CSF. (a) Morphology of seven-day cultured macrophages. (b–f) Flow cytometric determination of size and granularity (b) as well as surface expression of macrophage-specific markers CD163 (c), CD11c (d), CD206 (e), and CD68 (f). Representative histograms of  $n=4$  independent experiments are displayed. (g–l) Phagocytosis was determined as fluorescent intensity of pHrodo-labeled apoptotic cells (g, j), nucleosomes (h, k) and zymosan (l) in relation to calcein violet intensity (live cells). (i) For visualization, a representative fluorescent image of monocyte phagocytosis of pHrodo-zymosan is displayed. Data are means  $\pm$  SD of  $n=6$  individual donors.

Pathways regulated by FH treatment were identified using parametric analysis of gene-set enrichment. Canonical pathways from the KEGG and reactome databases were used as gene sets. Pathways that were most upregulated included those associated with monocyte differentiation and monocyte/macrophage function, such as

cytokine-cytokine receptor interactions, signaling pathway and ABC transporters. The type of upregulated pathways (IL-10 signaling; tryptophan, galactose and retinol metabolism as well as downregulation of IFN signaling and IFN- $\alpha$  response) strongly strengthens the hypothesis that FH-differentiation induces an immunosuppressive

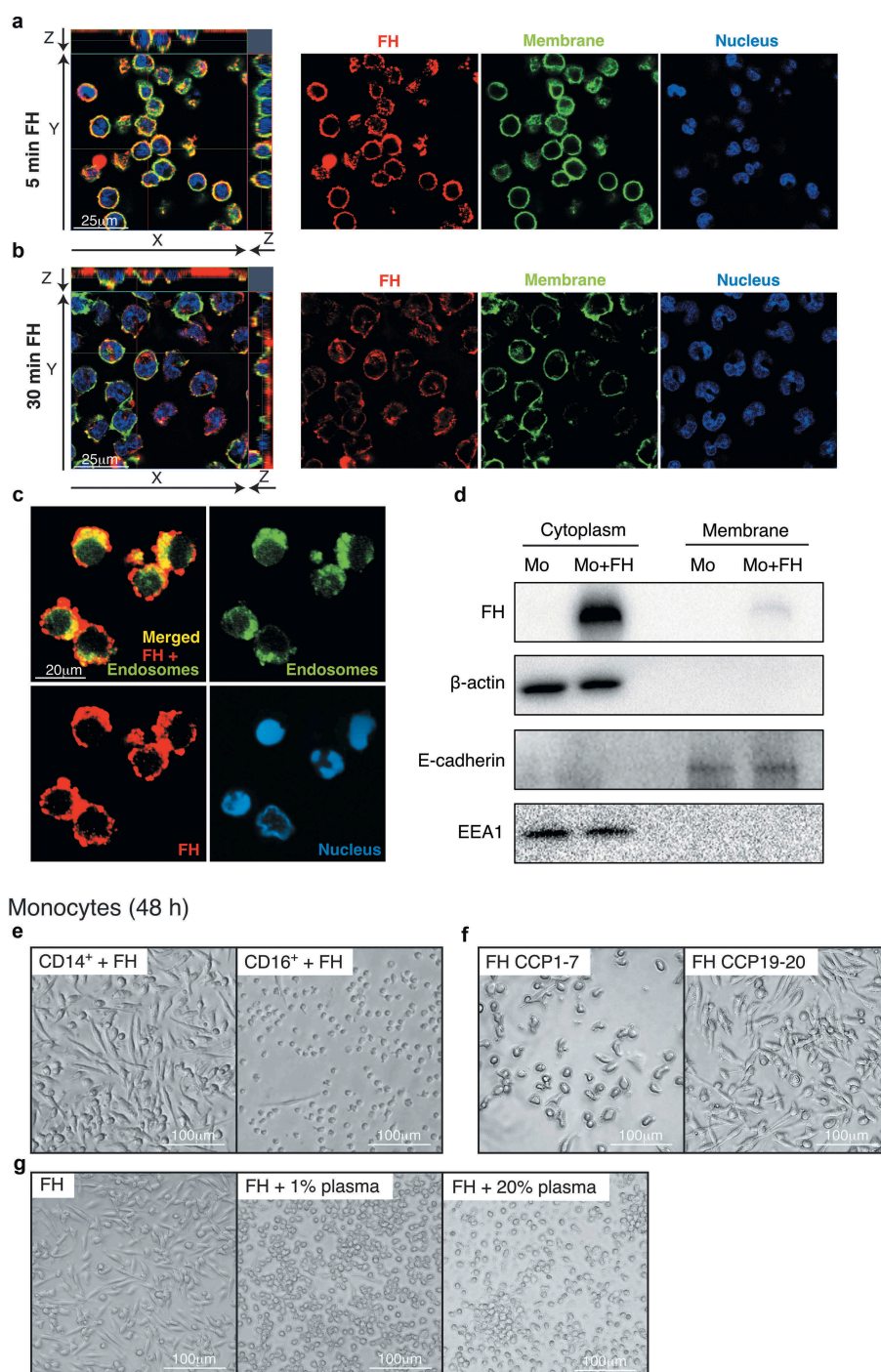


**Figure 3.** The morphological changes upon FH stimulation in CD14<sup>+</sup> monocytes are induced by CCP19-20 and are inhibited by plasma.

(a, b) Localization of FH was analyzed using confocal microscopy. Primary human CD14<sup>+</sup> monocytes were permeabilized after 5 min (a) or 30 min (b) incubation with 150  $\mu$ g/ml FH. The membrane was visualized with anti-CD44 Ab (green) and FH was detected with antiserum (red). The nuclei were counterstained with DAPI (blue). The confocal XY image with orthogonal YZ view. (c) FH at early stages of internalization is co-localized with endosomes. Primary human CD14<sup>+</sup> monocytes were permeabilized after 15 min incubation with 150  $\mu$ g/ml FH. The endosomes were detected with EEA1 Ab (green) and FH was detected with antiserum (red). Nuclei were counterstained with DAPI. (d) Internalization of FH was confirmed by fractionation of monocyte lysates incubated prior for 30 min with or without 150  $\mu$ g/ml biotinylated FH. Endosomes were detected in the same fraction with EEA1 antibody (e–g). Morphology of 48h cultured monocytes. CD14<sup>+</sup> and CD16<sup>+</sup> monocytes were purified with specific microbeads and incubated with 150  $\mu$ g/ml FH (e). CD14<sup>+</sup> monocytes were additionally incubated with the same molar concentration of FH CCP1-7 and CCP19-20 (f). Plasma effects were studied on monocytes stimulated with 150  $\mu$ g/ml full-length FH and supplemented with 1% and 20% autologous plasma (g). Mo – monocytes, Mo+FH – monocytes incubated with FH.

phenotype. Additional identified pathways included the activation of matrix metalloproteinases and collagen degradation, which are both engaged in ECM modification in cancer (Figure 4e).

### **FH alters cytokine profile**

The cytokine profile of monocytes upon 48 h stimulation with FH was compared to that of cells cultured without FH. At this

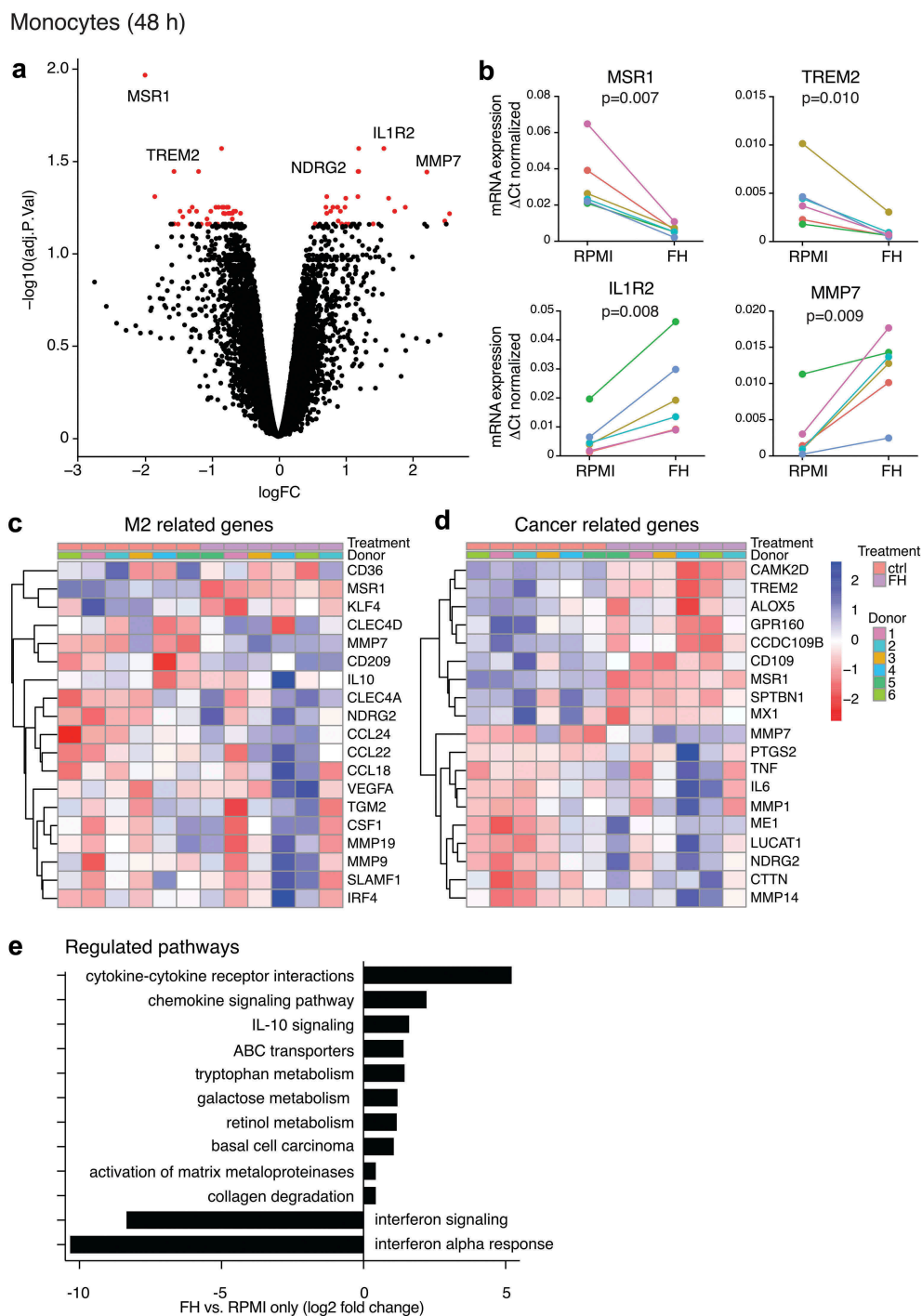


**Figure 4.** Transcriptome analysis of FH-stimulated monocytes.

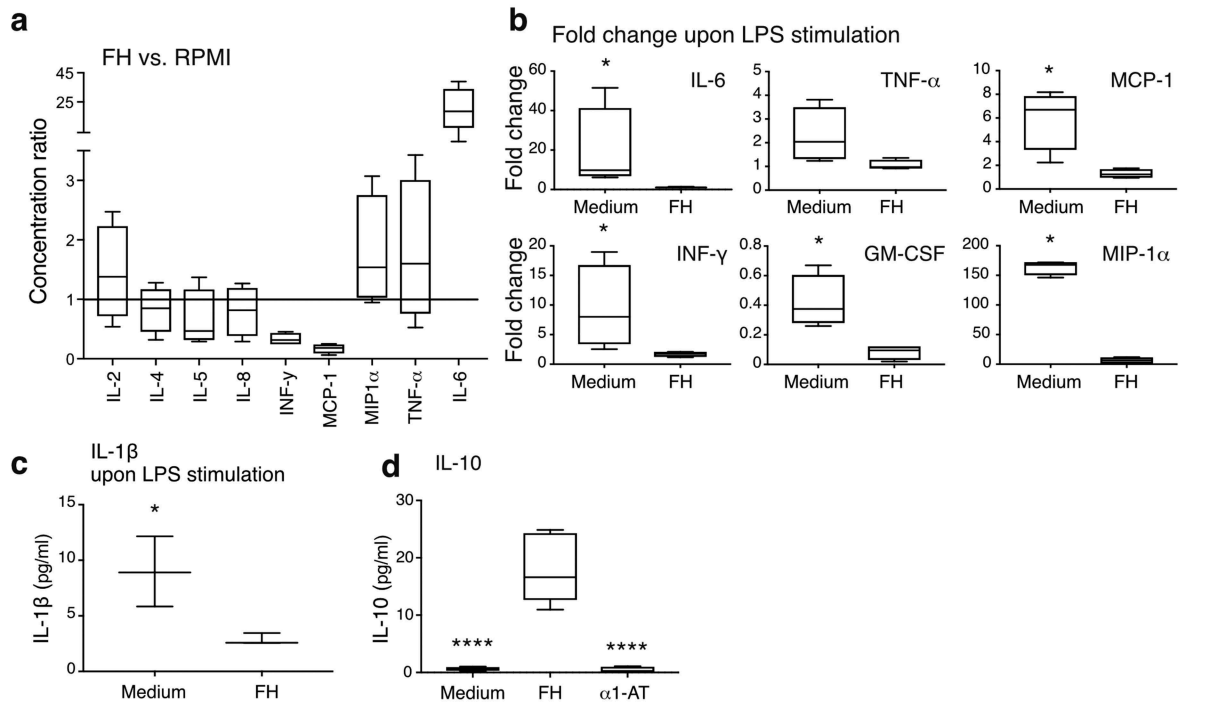
Affymetrix GeneChip expression profiling assay on primary human CD14<sup>+</sup> monocytes of six individual donors incubated for 48 h with RPMI medium or 150  $\mu$ g/ml FH. (a) Volcano plot of microarray data highlighting 70 genes with a nominal p-value <0.0001. Genes of interest that display both large magnitude fold-changes (x-axis) and high statistical significance ( $-\log_{10}$  of p-value, y-axis) are marked in red. (b) mRNA expression levels of four most regulated genes in six independent donors normalized to housekeeping gene. (c–d) Heat maps representing the most regulated genes involved in M2 polarization and cancer-associated macrophage function. (e) Highly regulated pathways involved in monocyte and macrophage function, differentiation, polarization and involvement in cancer pathology (e). Data of n=6 individual donors.

time point, RPMI-incubated monocytes remained viable (Figure 1b). IL-6 release was significantly increased by FH and a trend for elevated secretion of tumor necrosis factor- $\alpha$  (TNF- $\alpha$ ) and macrophage inflammatory protein 1- $\alpha$  (MIP-1 $\alpha$ ) was detected (Figure 5a). The release of other cytokines was unaltered. When LPS was added to the cultured

monocytes, it had a negligible effect on FH-treated cells, but significantly increased cytokine release in the RPMI control (Figure 5b). The release of pro-inflammatory IL-1 $\beta$  was significantly decreased in FH-treated cells upon additional LPS stimulation (Figure 5c). Remarkably, FH significantly increased the release of anti-inflammatory IL-10 after 48



## Monocytes (48 h)



## Macrophages (7 days)

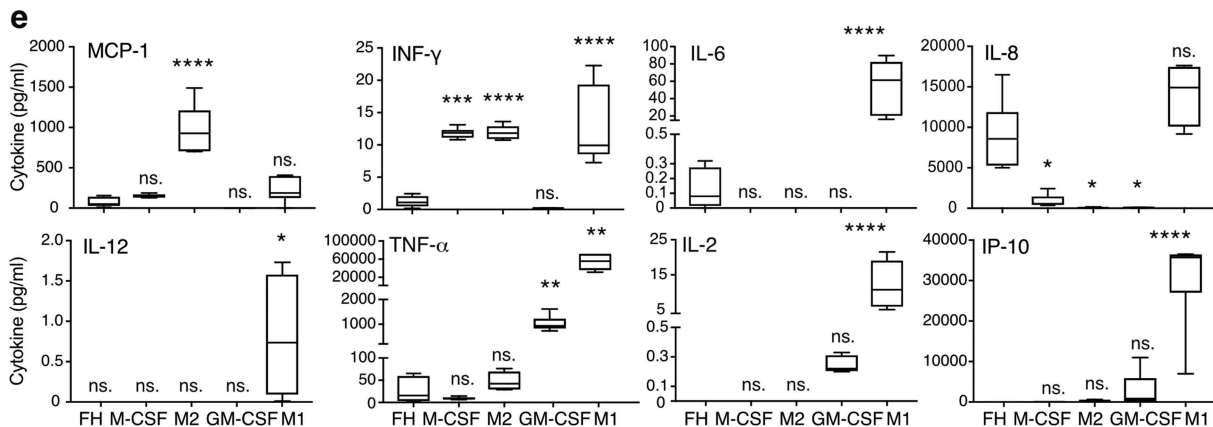


**Figure 5.** FH induces an anti-inflammatory cytokine release profile.

(a–d) CD14<sup>+</sup> monocytes were cultured for 48 h with medium, 150  $\mu$ g/ml FH or 150  $\mu$ g/ml  $\alpha$ 1-AT and further stimulated with 100 ng/ml LPS for the last 15 h (b and c). (e) Macrophages were differentiated for 7 days with 150  $\mu$ g/ml FH, 25 ng/ml M-CSF or 25 ng/ml GM-CSF. M1 and M2 macrophages were generated by additional incubation for 4 h with 100 ng/ml LPS or 20 ng/ml IL-4 and IL-13. (a–e) FH-rendered changes in cytokine release with (b, c) and without (a, d, e) LPS co-stimulation. Levels were determined with Bio-Plex Pro human cytokine 27-plex assay (a, b, e) or ELISA (c, d). Data are means  $\pm$  SD of n=4 (a, b), n=5 (d, e), and n=3 (c) individual donors. Significances (b–e) are calculated in comparison to FH.

h stimulation. The experiment included six donors out of which two were considered to be non-responders, based on lack of significant up-regulation upon M2 stimulation (data not shown). These donors were excluded from the graph (Figure 5d).

Cytokine changes upon seven-day stimulation were also investigated. Only M1 macrophages strongly secreted the proinflammatory cytokines IL-6, IL-12, TNF- $\alpha$  and interferon gamma-induced protein 10 (IP-10), whereas FH-induced macrophages produced negligible amounts, similar to M2 macrophages (Figure 5e). Consistent with Affymetrix data, FH-induced macrophages produced very low levels of IFN-

$\alpha$ . Noticeably, FH treatment increased the release of IL-8, a potentially tumor-promoting mediator and prognostic cancer biomarker (Figure 5e).<sup>35</sup>

### FH-induced macrophages are polarized into an immunosuppressive phenotype

To investigate further the role of FH in differentiation of monocytes into immunosuppressive macrophages, we compared the T-cell stimulating ability of seven-day cultured FH-induced macrophages with M-CSF and GM-CSF macrophages and medium-incubated monocytes. T-cell activation

was measured by assessing activation-induced clustering and proliferation after stimulation with bacterial superantigens, which mimic antigen presentation by nonspecifically cross-linking MHC class II proteins with the T-cell receptor. FH-induced macrophages supported a significantly lower level of T-cell proliferation than immunosuppressive and pro-inflammatory macrophages, in both tested concentrations of superantigens (Figure 6a). This was confirmed by significant differences in the size of T-cell clusters formed during coculture (Figure 6b). To understand the mechanism responsible for the poor ability of FH-induced macrophages to activate T-cells, we tested the expression of the co-inhibitory molecule programmed death-ligand 1 (PD-L1). The receptor for PD-L1, PD-1, is expressed on activated T-cells and downregulates activation.<sup>36</sup> FH-induced macrophages expressed significantly higher levels of PD-L1 than immunosuppressive and pro-inflammatory macrophages (Figure 6c), as well as medium-incubated cells (Figure S2F). Additionally, the MHC class II cell surface receptor HLA-DR expression was markedly reduced on FH-induced macrophages in comparison to other macrophages (Figure 6d). The expression of CD80 and CD86, which are ligands for T-cell co-stimulatory receptors, was also relatively low on FH-induced and

immunosuppressive macrophages in comparison to pro-inflammatory macrophages (Figure S2A).

Arginase metabolizes L-arginine and depletes it from the environment, which makes it relevant for the immunosuppressive function of macrophages. Differentiation of macrophages with FH also resulted in high arginase activity, which was surpassed only in fully polarized M2 macrophages (Figure 6e,f).

### **FH expression in breast cancer cells correlates with disease severity and M2 macrophage presence**

FH expression was investigated in a breast cancer patient cohort using immunochemistry. Specificity of anti-FH antibodies was verified using paraffin-embedded cell pellets of wild-type (WT) and FH-transfected HEK 293 cells (Figure 7a, Figure S3A, B). In patient tissues FH was expressed at varying levels by epithelial cancer cells, which is consistent with the previously detected expression of FH on mRNA level in breast cancer tissue ([www.proteinatlas.org/ENSG00000000971-CFH/pathology/breast+cancer#cbox](http://www.proteinatlas.org/ENSG00000000971-CFH/pathology/breast+cancer#cbox)) and various breast cancer cell lines.<sup>37</sup> The FH antiserum used in this study recognizes FH and FH splice variant FH-like protein (FHL1), due to the shared homology between FHL-1 and

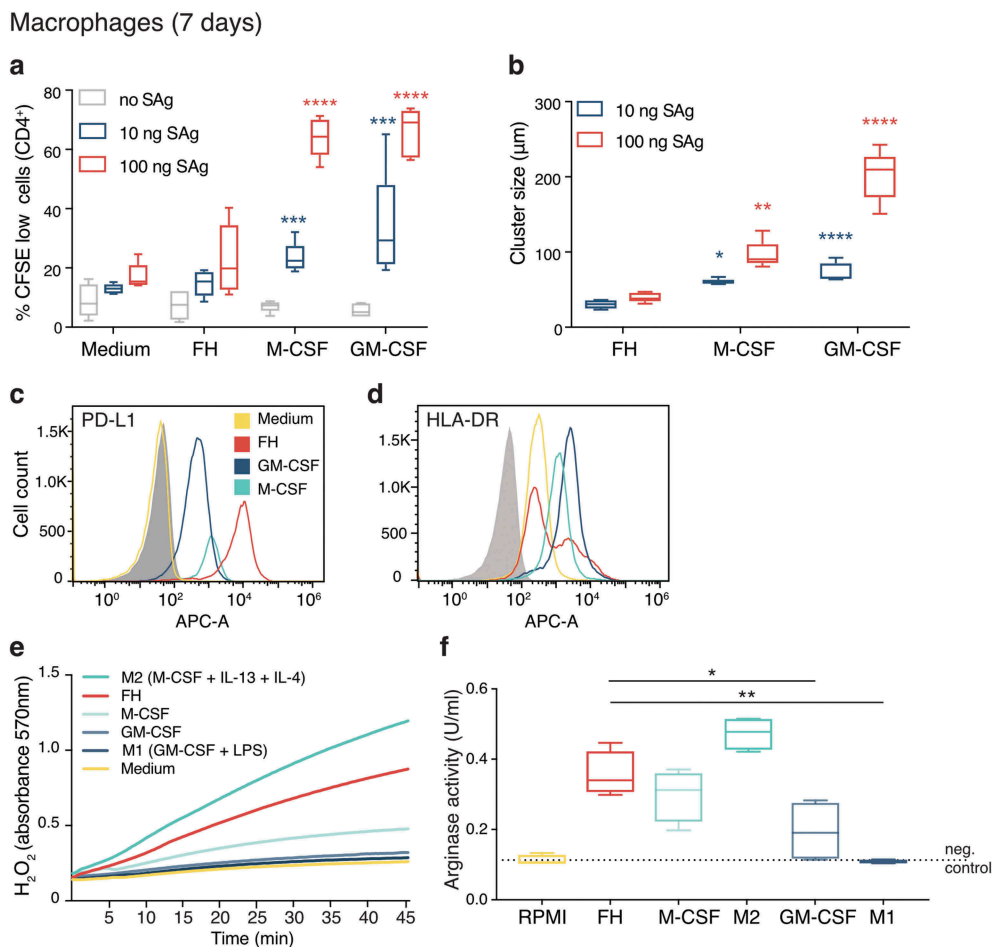


**Figure 6.** FH-induced macrophages exhibit a suppressive phenotype.

(a–f) Macrophages were differentiated for 7 days with 150 μg/ml FH, 25 ng/ml MCSF or 25 ng/ml GM-CSF. (e, f) M1 and M2 macrophages were generated by additional incubation for 4 h with 100 ng/ml LPS or 20 ng/ml IL-4 and IL-13. (a) Proliferation and (b) clusters size of autologous CFSE-labeled CD4<sup>+</sup> T-cells incubated for 3 days with macrophages stimulated with 10 or 100 ng of superantigens. (c–d) Flow cytometric determination of PD-L1 (c) and HLA-DR (d) surface expression. Representative histograms of n=4 independent experiments are displayed. (e) Kinetic and (f) endpoint measurement (45 min) of arginase activity were assessed by arginase activity assay kit. Data are means ± SD of n=5 (a, b) n=4 individual donors (e, f). Significances (a, b, f) were calculated in comparison to FH.

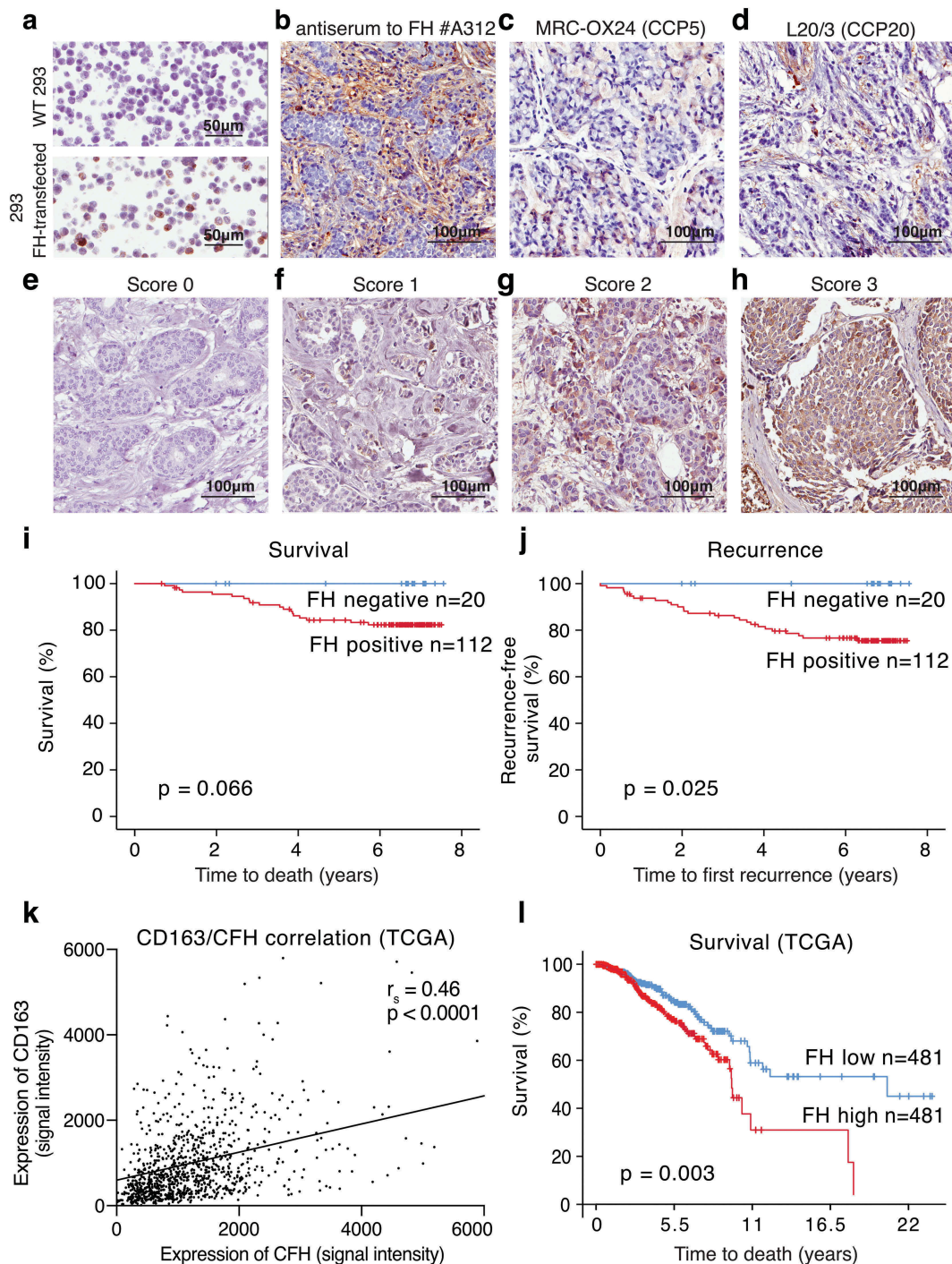


**Figure 7.** FH produced in breast tumors correlates with recurrence, disease severity and occurrence of M2 macrophages.

(a) Specificity of FH staining was determined in HEK 293 cells, transfected with FH or mock transfected. (b, c, d) Staining of FH in tissue microarrays (TMAs) from breast cancer patient cohort with antibodies recognizing different regions of the protein. (e, f, g, h) Scoring of FH levels in TMAs from breast cancer patient cohort. Representative pictures for each score at 40x magnification are presented. (i, j) Cancer-specific survival and recurrence-free survival associate with FH expression. Scores 1–3 were grouped as FH positive, score 0 was denoted as FH negative. (k) Analysis of correlation between FH expression and infiltration of CD163<sup>+</sup> macrophages in 1006 patient samples from the OncoLnc. (l) Confirmation of correlation between survival and FH expression using the TCGA database and SurvExpress search engine, based on the low or high risk for a poor outcome.

the seven N-terminal domains of FH. The antiserum also recognizes some of the FH-related proteins (FHRs), due to their homology with the C-terminal region of FH (Figure 7b). However, FHRs were not found in the breast tumors at the mRNA level.<sup>38</sup> To further confirm the specificity of our staining for FH, we stained selected breast cancer tissues with

MRC-OX24 antibody, which recognizes FH and FHL1 but not FHRs (Figure 7c) and L20/3, which recognizes FH and FHRs but not FHL1 (Figure 7d). Both of these antibodies yielded positive staining, which together with the data on mRNA expression strongly indicates that the protein detected in the tissue was indeed FH and not FHL1 or FHR.

In currently evaluated patient tissues, the staining intensity for FH in epithelial cancer cells was scored from 0 to 3 (Figure 7e–h). To create dichotomous variables, scores 1, 2 and 3 were denoted as FH positive and score 0 as FH negative. FH expression in tumors was modestly correlated with decreased overall survival (Figure 7i) and significantly with recurrence-free survival (Figure 7j). Judging each score separately, a clear dose–response was detected the higher FH expression, the poorer survival and more recurrence (Figure S3C, D). The intensity of FH expression in tumor cells was significantly associated with age at diagnosis, tumor size, Nottingham histological grade (NHG), proliferation (determined by KI-67 expression) and presence of M2 (CD163<sup>+</sup>) macrophages. No correlation was observed with nodal status, triple negative (Table 1), luminal A, luminal B, or basal subtype (data not shown). All clinical parameters were previously assessed for the same tissues.<sup>39</sup> Correlation of FH expression with infiltration of CD163<sup>+</sup> macrophages and correlation of FH expression with decreased survival were confirmed using OncoLnc database (<http://www.oncolnc.org>, Figure 7k) and TCGA database (breast invasive carcinoma project – July 2016) with SurvExpress (<http://bioinformatica.mty.itesm.mx:8080/Biomatec/SurvivaX.jsp>,<sup>40</sup> Figure 7l).

## Discussion

TAMs are important tumor-promoting cells in the breast tumor microenvironment and exert their action by, among others, inhibition of T-cell function, degradation of ECM, and stimulation of angiogenesis. Here, we show that FH is expressed by breast cancer cells and positively correlates with the presence of immunosuppressive macrophages. We further demonstrate that FH directly promotes differentiation of blood-derived monocytes into immunosuppressive macrophages.

While previously studying the effect of FH on nucleosome and apoptotic cell removal,<sup>19</sup> we unexpectedly observed changed morphology of monocytes in the presence of FH using serum-free medium. This prompted our current investigation, in which we explored the effect of FH on monocyte survival and differentiation. The mRNA expression profile of monocytes at early differentiation stages was altered significantly by FH and many strongly regulated genes define the role of macrophages in cancer and/or are associated with the ECM, which is an integral feature of tumors, contributing to tumor development. Noticeably, MMP7 was among the most regulated genes and consistently, MMPs and collagen degradation, which are both engaged in ECM modifications in the tumor

**Table 1.** Association between FH and clinical parameters.

Factor	n	FH intensity				p-value
		0	1	2	3	
All n (%)	132	20	44	50	18	
Age at diagnosis						<b>0.017</b>
Median		59	63	70	70	
(min, max)		(35, 81)	(34, 91)	(40, 97)	(51, 88)	
Size (tumor diameter, mm)						<b>&lt;0.0001</b>
Median		19	19	23	28	
(range)		(11,30)	(8, 145)	(11, 80)	(17, 140)	
NHG						<b>0.002</b>
I (%)	19	6	8	5	0	
II (%)	60	7	25	20	8	
III (%)	53	7	11	25	10	
Nodal status						0.172
0 (%)	68	11	21	29	7	
1-3 (%)	34	6	12	12	4	
4 (%)	19	1	5	6	7	
Missing	11					
ER status						0.082
Negative (%)	18	1	4	10	3	
Positive (%)	114	19	40	40	15	
PR status						0.167
Negative (%)	41	4	12	19	6	
Positive (%)	91	16	32	31	12	
HER2						0.117
Weak (%)	123	20	41	46	16	
Strong (%)	8	0	2	4	2	
Missing	1					
KI-67						<b>0.022</b>
0	5	1	4	0	0	
1	51	8	18	21	4	
2	60	9	13	26	12	
Missing	16					
Macrophages(CD68 <sup>+</sup> )						0.119
0	21	4	8	6	3	
1	50	7	19	19	5	
2	25	4	8	10	3	
3	7	0	0	5	2	
Missing	29					
M2 Macrophages (CD163 <sup>+</sup> )						<b>0.005</b>
0	29	4	15	7	3	
1	44	7	19	12	6	
2	21	3	4	12	2	
3	9	0	0	6	3	
Missing	29					

Abbreviations: FH, factor H; ER, estrogen receptor; HER2, human epidermal growth factor receptor 2; NGH, Nottingham histological grade; PR, progesterone receptor. Spearman correlation, two-tailed P-value. The bold indicates P-values <0.05.

microenvironment, were among the most upregulated pathways. The fact that the expression of matrix modulating proteins such as collagen cross-linkers and MMPs is predictive of poor prognosis in breast cancer patients<sup>41</sup> suggests that FH-derived macrophages influence breast cancer severity and prognosis by modulating the ECM.

Many other altered genes are associated with macrophage activation and polarization.<sup>42-46</sup> Among these, numerous M2-related genes were upregulated. Changes in tryptophan and arginine metabolism also suggest that FH promotes an immunosuppressive phenotype. Upregulation of tryptophan metabolism impairs T-cell proliferation. Consequently, the ability of T-cells to kill pathogens and cancer cells is inhibited.<sup>47</sup> Arginine depletion also affects T-cells in a similar way, which is well documented in *in vivo* studies.<sup>48</sup> In man, many reports document arginase activity in monocytes and macrophages, while others do not. One of the reasons for this controversy might be the usage of different models and detection methods, with measurement of arginase activity being much more sensitive than direct detection of arginase expression.<sup>49</sup> In our experimental setup, human macrophages stimulated with M2 stimuli as well as with FH showed relatively high arginase activity.

At later differentiation stages, FH-induced macrophages expressed much higher levels of PD-L1 than other tested macrophages. PD-L1 and its receptor PD-1 that is expressed on activated T-cells act together as co-inhibitory factors, which can limit T-cell responses to ensure that the immune system is only activated when appropriate. Noticeably, immunosuppressive macrophages have emerged as important modulators of PD-1 activity and PD-1/PD-L1 immune checkpoint inhibitors have good therapeutic effect in breast cancer patients.<sup>50</sup> Thus, one can hypothesize that FH-expressing breast tumors may better respond to PD-1/PD-L1 inhibitors. Although there is not much known about the role of PD-1/PD-L1 in superantigen presentation, one study showed that blocking PD-1 promotes T-cell responses in staphylococcal enterotoxin B-stimulated PBMCs.<sup>51</sup> The high expression of PD-L1 as well as the low expression of HLA-DR might therefore explain the T-cell suppressing effects observed in FH-induced macrophages upon stimulation with superantigens. Based on the low expression of HLA-DR, CD80 and CD86, one can hypothesize that FH might have similar inhibitory effects in the scenario of classical antigen presentation.

FH increased anti-inflammatory IL-10 and decreased most pro-inflammatory cytokines, most notably IFN- $\gamma$  and GM-CSF, creating an anti-inflammatory environment, while inhibiting M1 differentiation. Surprisingly IL-8, which is associated with metastatic dissemination, worse prognosis and attraction of immunosuppressive cells to cancer microenvironment was upregulated.<sup>52,53</sup> Our data are supported by the results of another study showing similar changes in the cytokine release profile and resistance to LPS by dendritic cells stimulated with FH.<sup>22</sup> This suggests changes in CD14 receptor signaling, either by direct binding of FH or indirect modifications, especially since the observed effects of FH are only pronounced in CD14<sup>+</sup> monocytes.

Further, the morphology and surface marker expression of FH-induced macrophages were similar to immunosuppressive macrophages. CD206 is expressed by several types of tissue resident macrophages and TAMs<sup>54-57</sup> and it is highly amplified by GM-CSF and TGF- $\beta$ .<sup>58</sup> CD206 may play a role in the

resolution of inflammation, since the lack of its expression is concurrent with elevated levels of inflammatory proteins in serum.<sup>59</sup> CD163 is commonly used as marker of an immunosuppressive phenotype in the macrophage polarization continuum.<sup>8</sup> CD163 is upregulated by M-CSF and highly expressed by TAMs. In breast cancer, CD163 has been correlated with early recurrence and reduced patient survival.<sup>13,60</sup> FH-induced macrophages co-express CD163 and CD206, indicating an immunosuppressive and regulatory phenotype similar to classically defined M2 and TAMs. Additionally, our data also support previous findings that CD206<sup>+</sup>/CD163<sup>+</sup> macrophages exhibit an increased capability for early apoptotic cell clearance.<sup>61</sup> We and others have reported previously that the FH-opsonization of targets facilitates their removal.<sup>19,62,63</sup> However, the role of FH as a stimulant for phagocytes is controversial. One study showed that pre-incubation of monocytes with FH inhibits C1q-enhanced uptake of apoptotic cells, while no effect of FH alone was detected.<sup>64</sup> Another report revealed a significant decrease in phagocytosis of apoptotic cells when incubated with FH from lupus nephritis patients with single amino acid substitution polymorphisms in FH, in comparison to FH from healthy donors.<sup>65</sup> Both studies employed short (2 h) incubations of the phagocytes with FH. In contrast, in our experiments, where we detected increased phagocytosis of apoptotic cells, phagocytes were stimulated much longer (2 and 7 days), allowing differentiation, which may explain the discrepancy.

In summary, we demonstrate that FH plays a role in the modulation of the tumor microenvironment in breast cancer. We propose that FH produced by tumor cells induces differentiation of macrophages into an immunosuppressive subtype that suppresses the immune system via several mechanisms, including changes in cytokine release and metabolism, as well as inhibition of T-cell responses. Immunosuppressive changes in the microenvironment, mediated by FH, should be taken into consideration to increase the effectiveness of immunotherapies against breast cancer.

## Acknowledgments

We thank Dr Peter Storm for the bioinformatic analyses, Dr Ben King, Lund University, for discussions and language revision of the manuscript and Mrs Ekström-Holka for help with immunochemical stainings.



## Disclosure of potential conflicts of interest

No potential conflicts of interest were disclosed.

## Funding

This study was supported by the Swedish Research Council [2016-01142 and 2018-02392], Cancerfonden, Foundations of Österlund, King Gustav V's 80th Anniversary, Knut and Alice Wallenberg, and grants for clinical research (ALF and the Skåne University Hospital).

## ORCID

Karolina I. Smolag  <http://orcid.org/0000-0001-6940-7130>  
Catharina Hagerling  <http://orcid.org/0000-0001-5631-7988>  
Anna M. Blom  <http://orcid.org/0000-0002-1348-1734>

## References

1. Yona S, Kim K-W, Wolf Y, Mildner A, Varol D, Breker M, Strauss-Ayali D, Viukov S, Williams M, Misharin A, et al. Fate mapping reveals origins and dynamics of monocytes and tissue macrophages under homeostasis. *Immunity*. 2013;38(1):79–91. doi:10.1016/j.immuni.2012.12.001.
2. Jakubzick C, Gautier EL, Gibbings SL, Sojka DK, Schlitzer A, Johnson TE, Ivanov S, Duan Q, Bala S, Condon T, et al. Minimal differentiation of classical monocytes as they survey steady-state tissues and transport antigen to lymph nodes. *Immunity*. 2013;39(3):599–610. doi:10.1016/j.immuni.2013.08.007.
3. Liu K, Waskow C, Liu X, Yao K, Hoh J, Nussenzweig M. Origin of dendritic cells in peripheral lymphoid organs of mice. *Nat Immunol*. 2007;8(6):578–583. doi:10.1038/ni1462.
4. Biswas SK, Mantovani A. Macrophage plasticity and interaction with lymphocyte subsets: cancer as a paradigm. *Nat Immunol*. 2010;11(10):889–896. doi:10.1038/ni.1937.
5. MacMicking J, Xie QW, Nathan C. Nitric oxide and macrophage function. *Annu Rev Immunol*. 1997;15:323–350. doi:10.1146/annurev.immunol.15.1.323.
6. Martinez FO, Gordon S. The M1 and M2 paradigm of macrophage activation: time for reassessment. *F1000Prime Rep*. 2014;6:13. doi:10.12703/P.
7. Taylor PR, Pickering MC, Kosco-Vilbois MH, Walport MJ, Botto M, Gordon S, Martinez-Pomares L. The follicular dendritic cell restricted epitope, FDC-M2, is complement C4; localization of immune complexes in mouse tissues. *Eur J Immunol*. 2002;32(7):1883–1896. doi:10.1002/1521-4141(200207)32:7<1883::AID-IMMU1888>3.0.CO;2-8.
8. Murray PJ, Allen JE, Biswas SK, Fisher EA, Gilroy DW, Goerdjt S, Gordon S, Hamilton J, Ivashkiv L, Lawrence T. Macrophage activation and polarization: nomenclature and experimental guidelines. *Immunity*. 2014;41(1):14–20. doi:10.1016/j.immuni.2014.06.008.
9. Leek RD, Lewis CE, Whitehouse R, Greenall M, Clarke J, Harris AL. Association of macrophage infiltration with angiogenesis and prognosis in invasive breast carcinoma. *Cancer Res*. 1996;56:4625–4629.
10. Ostrand-Rosenberg S, Sinha P. Myeloid-derived suppressor cells: linking inflammation and cancer. *J Immunol*. 2009;182(8):4499–4506. doi:10.4049/jimmunol.0802740.
11. Conklin MW, Keely PJ. Why the stroma matters in breast cancer: insights into breast cancer patient outcomes through the examination of stromal biomarkers. *Cell Adh Migr*. 2012;6(3):249–260. doi:10.4161/cam.20567.
12. Pollard JW. Macrophages define the invasive microenvironment in breast cancer. *J Leukoc Biol*. 2008;84(3):623–630. doi:10.1189/jlb.1107762.
13. Medrek C, Ponten F, Jirstrom K, Leandersson K. The presence of tumor associated macrophages in tumor stroma as a prognostic marker for breast cancer patients. *BMC Cancer*. 2012;12:306. doi:10.1186/1471-2407-12-306.
14. Junnikkala S, Hakulinen J, Jarva H, Manuelian T, Bjorge L, Butzow R, Zipfel PF, Meri S. Secretion of soluble complement inhibitors factor H and factor H-like protein (FHL-1) by ovarian tumour cells. *Br J Cancer*. 2002;87(10):1119–1127. doi:10.1038/sj.bjc.6600614.
15. Ajona D, Castano Z, Garayoa M, Zudaire E, Pajares MJ, Martinez A, Cuttitta F, Montuenga LM, Pio R. Expression of complement factor H by lung cancer cells: effects on the activation of the alternative pathway of complement. *Cancer Res*. 2004;64(17):6310–6318. doi:10.1158/0008-5472.CAN-03-2328.
16. Ohtsuka H, Imamura T, Matsushita M, Tanase S, Okada H, Ogawa M, Kambara T. Thrombin generates monocyte chemotactic activity from complement factor H. *Immunology*. 1993;80:140–145.
17. Hartung HP, Hadding U, Bitter-Suermann D, Gerns D. Release of prostaglandin E and thromboxane from macrophages by stimulation with factor H. *Clin Exp Immunol*. 1984;56:453–458.
18. Calippe B, Augustin S, Beguier F, Charles-Messance H, Poupel L, Conart J-B, Hu SJ, Lavalette S, Fauvet A, Rayes J. Complement factor H inhibits CD47-mediated resolution of inflammation. *Immunity*. 2017;46(2):261–272. doi:10.1016/j.immuni.2017.01.006.
19. Martin M, Leffler J, Smolag KI, Mytych J, Bjork A, Chaves LD, Alexander JJ, Quigg RJ, Blom AM. Factor H uptake regulates intracellular C3 activation during apoptosis and decreases the inflammatory potential of nucleosomes. *Cell Death Differ*. 2016;23(5):903–911. doi:10.1038/cdd.2015.164.
20. Blom AM, Kask L, Dahlback B. CCP1-4 of the C4b-binding protein alpha-chain are required for factor I mediated cleavage of complement factor C3b. *Mol Immunol*. 2003;39(10):547–556. doi:10.1016/S0161-5890(02)00213-4.
21. Laurell CB, Dahlqvist I, Persson U. The use of thiol-disulphide exchange chromatography for the automated isolation of alpha 1-antitrypsin and other plasma proteins with reactive thiol groups. *J Chromatogr*. 1983;278(1):53–61. doi:10.1016/S0378-4347(00)84755-6.
22. Olivar R, Luque A, Cardenas-Brito S, Naranjo-Gomez M, Blom AM, Borrás FE, Rodriguez de Córdoba S, Zipfel PF, Aran JM. The complement inhibitor factor h generates an anti-inflammatory and tolerogenic state in monocyte-derived dendritic cells. *J Immunol*. 2016;196(10):4274–4290. doi:10.4049/jimmunol.1500455.
23. Schmidt CQ, Herbert AP, Kavanagh D, Gandy C, Fenton CJ, Blaum BS, Lyon M, Uhrin D, Barlow PN. A new map of glycosaminoglycan and C3b binding sites on factor H. *J Immunol*. 2008;181(4):2610–2619. doi:10.4049/jimmunol.181.4.2610.
24. Vandesompele J, De Preter K, Pattyn F, Poppe B, Van Roy N, De Paepe A, Speleman F. Accurate normalization of real-time quantitative RT-PCR data by geometric averaging of multiple internal control genes. *Genome Biol*. 2002;3(7):RESEARCH0034. doi:10.1186/gb-2002-3-7-research0034.
25. Irizarry RA, Bolstad BM, Collin F, Cope LM, Hobbs B, Speed TP. Summaries of Affymetrix GeneChip probe level data. *Nucleic Acids Res*. 2003;31(4):e15. doi:10.1093/nar/gng015.
26. Benjamini Y, Hochberg Y. Controlling the false discovery rate - a practical and powerful approach to multiple testing. *J Roy Stat Soc B Met*. 1995;57:289–300.
27. Luo W, Friedman MS, Shedden K, Hankenson KD, Woolf PJ. GAGE: generally applicable gene set enrichment for pathway analysis. *BMC Bioinformatics*. 2009;10:161. doi:10.1186/1471-2105-10-161.
28. Svensson KJ, Christianson HC, Kucharzewska P, Fagerstrom V, Lundstedt L, Borgquist S, et al. Chondroitin sulfate expression predicts poor outcome in breast cancer. *Int J Oncol*. 2011;39(6):1421–1428. doi:10.3892/ijo.2011.1164.
29. Borgquist S, Jogi A, Ponten F, Ryden L, Brennan DJ, Jirstrom K. Prognostic impact of tumour-specific HMG-CoA reductase expression in primary breast cancer. *Breast Cancer Res*. 2008;10(5):R79. doi:10.1186/bcr2146.
30. Borgquist S, Holm C, Stendahl M, Anagnostaki L, Landberg G, Jirstrom K. Oestrogen receptors alpha and beta show different associations to clinicopathological parameters and their co-expression might predict a better response to endocrine treatment in breast cancer. *J Clin Pathol*. 2008;61(2):197–203. doi:10.1136/jcp.2006.040378.
31. Bayik D, Tross D, Haile LA, Verthelyi D, Klinman DM. Regulation of the maturation of human monocytes into immunosuppressive macrophages. *Blood Adv*. 2017;1(26):2510–2519. doi:10.1182/bloodadvances.2017011221.
32. EMMFJVJA ATEN. Measurement of co-localization of objects in dual-colour confocal images. *J Microsc*. 1993;169:375–382. doi:10.1111/j.1365-2818.1993.tb03313.x.
33. Ferreira VP, Herbert AP, Hocking HG, Barlow PN, Pangburn MK. Critical role of the C-terminal domains of factor H in regulating complement activation at cell surfaces. *J Immunol*. 2006;177(9):6308–6316. doi:10.4049/jimmunol.177.9.6308.
34. Oppermann M, Manuelian T, Jozsi M, Brandt E, Jokiranta TS, Heinen S, Meri S, Skerka C, Gotze O, Zipfel PF. The C-terminus of complement regulator Factor H mediates target recognition: evidence for a compact conformation of the native protein. *Clin Exp Immunol*. 2006;144(2):342–352. doi:10.1111/cei.2006.144.issue-2.
35. Kotyza J. Interleukin-8 (CXCL8) in tumor associated non-vascular extracellular fluids: its diagnostic and prognostic values. A review *Int J Biol Markers*. 2012;27(3):169–178. doi:10.5301/IJBM.2012.9261.

36. Parry RV, Chemnitz JM, Frauwirth KA, Lanfranco AR, Braunstein I, Kobayashi SV, Linsley PS, Thompson CB, Riley JL. CTLA-4 and PD-1 receptors inhibit T-cell activation by distinct mechanisms. *Mol Cell Biol.* 2005;25(21):9543–9553. doi:10.1128/MCB.25.21.9543-9553.2005.
37. Ringner M, Fredlund E, Hakkinen J, Borg A, Staaf J. GOBO: gene expression-based outcome for breast cancer online. *PLoS One.* 2011;6(3):e17911. doi:10.1371/journal.pone.0017911.
38. Uhlen M, Zhang C, Lee S, Sjostedt E, Fagerberg L, Bidkhorji G, Benfeitas R, Arif M, Liu Z, Edfors F. A pathology atlas of the human cancer transcriptome. *Science.* 2017;357:6352. doi:10.1126/science.aan2507.
39. Lundgren S, Karnevi E, Elebro J, Nodin B, Karlsson MCI, Eberhard J, Leandersson K, Jirstrom K. The clinical importance of tumour-infiltrating macrophages and dendritic cells in periampullary adenocarcinoma differs by morphological subtype. *J Transl Med.* 2017;15(1):152. doi:10.1186/s12967-017-1256-y.
40. Aguirre-Gamboa R, Gomez-Rueda H, Martinez-Ledesma E, Martinez-Torteya A, Chacolla-Huaringa R, Rodriguez-Barrientos A, Tamez-Peña JG, Treviño V. SurvExpress: an online biomarker validation tool and database for cancer gene expression data using survival analysis. *PLoS One.* 2013;8(9):e74250. doi:10.1371/journal.pone.0074250.
41. Slattery ML, John E, Torres-Mejia G, Stern M, Lundgreen A, Hines L, Giuliano A, Baumgartner K, Herrick J, Wolff RK. Matrix metalloproteinase genes are associated with breast cancer risk and survival: the Breast Cancer Health Disparities Study. *PLoS One.* 2013;8(5):e63165. doi:10.1371/journal.pone.0063165.
42. Krakowiak MS, Noto JM, Piauzelo MB, Hardbower DM, Romero-Gallo J, Delgado A, Chaturvedi R, Correa P, Wilson KT, Peek RM, et al. Matrix metalloproteinase 7 restrains Helicobacter pylori-induced gastric inflammation and premalignant lesions in the stomach by altering macrophage polarization. *Oncogene.* 2015;34(14):1865–1871. doi:10.1038/onc.2014.135.
43. Huang WC, Sala-Newby GB, Susana A, Johnson JL, Newby AC. Classical macrophage activation up-regulates several matrix metalloproteinases through mitogen activated protein kinases and nuclear factor-kappaB. *PLoS One.* 2012;7(8):e42507. doi:10.1371/journal.pone.0042507.
44. Choi SC, Kim KD, Kim JT, Oh SS, Yoon SY, Song EY, Lee HG, Choe Y-K, Choi I, Lim J-S, et al. NDRG2 is one of novel intrinsic factors for regulation of IL-10 production in human myeloid cell. *Biochem Biophys Res Commun.* 2010;396(3):684–690. doi:10.1016/j.bbrc.2010.04.162.
45. Li M, Lai X, Zhao Y, Zhang Y, Li M, Li D, Kong J, Zhang Y, Jing P, Li H, et al. Loss of NDRG2 in liver microenvironment inhibits cancer liver metastasis by regulating tumor associated macrophages polarization. *Cell Death Dis.* 2018;9(2):248. doi:10.1038/s41419-018-0284-8.
46. Turnbull IR, Gilfillan S, Cella M, Aoshi T, Miller M, Piccio L, Hernandez M, Colonna M. Cutting edge: TREM-2 attenuates macrophage activation. *J Immunol.* 2006;177(6):3520–3524. doi:10.4049/jimmunol.177.6.3520.
47. Mellor AL, Baban B, Chandler P, Marshall B, Jhaver K, Hansen A, Koni PA, Iwashima M, Munn DH. Cutting edge: induced indoleamine 2,3 dioxygenase expression in dendritic cell subsets suppresses T cell clonal expansion. *J Immunol.* 2003;171(4):1652–1655. doi:10.4049/jimmunol.171.4.1652.
48. Bronte V, Zanovello P. Regulation of immune responses by L-arginine metabolism. *Nat Rev Immunol.* 2005;5(8):641–654. doi:10.1038/nri1668.
49. Thomas AC, Mattila JT. “Of mice and men”: arginine metabolism in macrophages. *Front Immunol.* 2014;5:479. doi:10.3389/fimmu.2014.00479.
50. Bertucci F, Goncalves A. Immunotherapy in Breast Cancer: the Emerging Role of PD-1 and PD-L1. *Curr Oncol Rep.* 2017;19(10):64. doi:10.1007/s11912-017-0627-0.
51. Wang C, Thudium KB, Han M, Wang X-T, Huang H, Feingersh D, Garcia C, Wu Y, Kuhne M, Srinivasan M. In vitro characterization of the anti-PD-1 antibody nivolumab, BMS-936558, and in vivo toxicology in non-human primates. *Cancer Immunol Res.* 2014;2(9):846–856. doi:10.1158/2326-6066.CIR-14-0040.
52. Balkwill F. Cancer and the chemokine network. *Nat Rev Cancer.* 2004;4(7):540–550. doi:10.1038/nrc1388.
53. Alfaro C, Sanmamed MF, Rodriguez-Ruiz ME, Teijeira A, Onate C, Gonzalez A, Ponz M, Schalper KA, Pérez-Gracia JL, Melero I, et al. Interleukin-8 in cancer pathogenesis, treatment and follow-up. *Cancer Treat Rev.* 2017;60:24–31. doi:10.1016/j.ctrv.2017.08.004.
54. Zeyda M, Farmer D, Todoric J, Aszmann O, Speiser M, Gyori G, Zlabinger GJ, Stulnig TM. Human adipose tissue macrophages are of an anti-inflammatory phenotype but capable of excessive pro-inflammatory mediator production. *Int J Obes (Lond).* 2007;31(9):1420–1428. doi:10.1038/sj.ijo.0803632.
55. Aron-Wisnewsky J, Tordjman J, Poitou C, Darakhshan F, Hugol D, Basdevant A, Aissat A, Guerre-Millo M, Clément K. Human adipose tissue macrophages: m1 and m2 cell surface markers in subcutaneous and omental depots and after weight loss. *J Clin Endocrinol Metab.* 2009;94(11):4619–4623. doi:10.1210/jc.2009-0925.
56. Titos E, Rius B, Gonzalez-Periz A, Lopez-Vicario C, Moran-Salvador E, Martinez-Clemente M, Arroyo V, Clària J. Resolvin D1 and its precursor docosahexaenoic acid promote resolution of adipose tissue inflammation by eliciting macrophage polarization toward an M2-like phenotype. *J Immunol.* 2011;187(10):5408–5418. doi:10.4049/jimmunol.1100225.
57. Svensson-Arvelund J, Mehta RB, Lindau R, Mirrasekhian E, Rodriguez-Martinez H, Berg G, Lash GE, Jenmalm MC, Ernerudh J. The human fetal placenta promotes tolerance against the semiallogeneic fetus by inducing regulatory T cells and homeostatic M2 macrophages. *J Immunol.* 2015;194(4):1534–1544. doi:10.4049/jimmunol.1401536.
58. Dupasquier M, Stoitznier P, Wan H, Cerqueira D, van Oudenaren A, Voerman JS, Denda-Nagai K, Irimura T, Raes G, Romani N. The dermal microenvironment induces the expression of the alternative activation marker CD301/mMGL in mononuclear phagocytes, independent of IL-4/IL-13 signaling. *J Leukoc Biol.* 2006;80(4):838–849. doi:10.1189/jlb.1005564.
59. Lee SJ, Evers S, Roeder D, Parlow AF, Risteli J, Risteli L, et al. Mannose receptor-mediated regulation of serum glycoprotein homeostasis. *Science.* 2002;295(5561):1898–1901. doi:10.1126/science.1069540.
60. Shabo I, Stal O, Olsson H, Dore S, Svanvik J. Breast cancer expression of CD163, a macrophage scavenger receptor, is related to early distant recurrence and reduced patient survival. *Int J Cancer.* 2008;123(4):780–786. doi:10.1002/ijc.23527.
61. Zizzo G, Hilliard BA, Monestier M, Cohen PL. Efficient clearance of early apoptotic cells by human macrophages requires M2c polarization and MerTK induction. *J Immunol.* 2012;189(7):3508–3520. doi:10.4049/jimmunol.1200662.
62. Haapasalo K, Jarva H, Siljander T, Tewodros W, Vuopio-Varkila J, Jokiranta TS. Complement factor H allotype 402H is associated with increased C3b opsonization and phagocytosis of Streptococcus pyogenes. *Mol Microbiol.* 2008;70(3):583–594. doi:10.1111/mmi.2008.70.issue-3.
63. Abdul-Aziz M, Tsolaki AG, Kouser L, Carroll MV, Al-Ahdal MN, Sim RB, Kishore U. Complement factor H interferes with Mycobacterium bovis BCG entry into macrophages and modulates the pro-inflammatory cytokine response. *Immunobiology.* 2016;221(9):944–952. doi:10.1016/j.imbio.2016.05.011.
64. Kang YH, Urban BC, Sim RB, Kishore U. Human complement Factor H modulates C1q-mediated phagocytosis of apoptotic cells. *Immunobiology.* 2012;217(4):455–464. doi:10.1016/j.imbio.2011.10.008.
65. Wang FM, Song D, Pang Y, Song Y, Yu F, Zhao MH. The dysfunctions of complement factor H in lupus nephritis. *Lupus.* 2016;25(12):1328–1340. doi:10.1177/0961203316642307.